UNCLASSIFIED
SECURITY CLASSIFICATION OF THIS PAGE

MASTER COPY - FOR REPRODUCTION PURPOSES

REPORT DOCUMENTATION PAGE

1a. AD-A213 514

1b. RESTRICTIVE MARKINGS

3. DISTRIBUTION/AVAILABILITY OF REPORT
Approved for public release; distribution unlimited.

4. PERFORMING ORGANIZATION REPORT NUMBER(S)

5. MONITORING ORGANIZATION REPORT NUMBER(S)
ARO 26049.2-CH

6a. NAME OF PERFORMING ORGANIZATION
Chemistry Department
University of Wisconsin

6b. OFFICE SYMBOL (If applicable)

7a. NAME OF MONITORING ORGANIZATION
U. S. Army Research Office

6c. ADDRESS (City, State, and ZIP Code)
1101 University Avenue
Madison, Wisconsin 53706

7b. ADDRESS (City, State, and ZIP Code)
P. O. Box 12211
Research Triangle Park, NC 27709-2211

8a. NAME OF FUNDING/SPONSORING ORGANIZATION
U. S. Army Research Office

8b. OFFICE SYMBOL (If applicable)

9. PROCUREMENT INSTRUMENT IDENTIFICATION NUMBER

8c. ADDRESS (City, State, and ZIP Code)
P. O. Box 12211
Research Triangle Park, NC 27709-2211

10. SOURCE OF FUNDING NUMBERS

PROGRAM ELEMENT NO.	PROJECT NO.	TASK NO.	WORK UNIT ACCESSION NO.

11. TITLE (Include Security Classification)
The vibrationally mediated photodissociation dynamics of nitric acid

12. PERSONAL AUTHOR(S)
Amitabha Sinha, Randall L. Vander Wal and F. Fleming Crim

13a. TYPE OF REPORT	13b. TIME COVERED FROM ____ TO ____	14. DATE OF REPORT (Year, Month, Day)	15. PAGE COUNT
Reprint			

16. SUPPLEMENTARY NOTATION
The view, opinions and/or findings contained in this report are those of the author(s) and should not be construed as an official Department of the Army position, policy, or decision, unless so designated by other documentation.

17. COSATI CODES		
FIELD	GROUP	SUB-GROUP

18. SUBJECT TERMS (Continue on reverse if necessary and identify by block number)
molecular decomposition, photodissociation, vibrational excitation

19. ABSTRACT (Continue on reverse if necessary and identify by block number)

Vibrationally mediated photodissociation, in which one photon prepares a highly vibrationally excited molecule by vibrational overtone excitation and a second photon dissociates the vibrationally excited molecule, is a means of studying the spectroscopy and photodissociation dynamics of highly vibrationally excited states. Applying this dissociation scheme to nitric acid ($HONO_2$) excited in the region of the third overtone of the O-H stretching vibration (ν_{OH}) and detecting the OH fragment by laser induced fluorescence determines the energy partitioning and identifies the influence of vibrational excitation prior to dissociation. Vibrationally mediated photodissociation using 755 and 355 nm photons deposits *more* energy in relative translation than the isoenergetic single photon dissociation with 241 nm light. The former process also produces three times more vibrationally excited OH fragments, and both processes form electronically excited NO_2, which receives over three-quarters of the available energy. In these experiments, vibrational overtone excitation enhances the cross section for the electronic transition by about three orders of magnitude. The observed differences are consistent with the motion of the vibrationally excited molecule on the ground electronic state surface strongly influencing the dissociation dynamics by allowing access to different electronic states in the photolysis step.

20. DISTRIBUTION/AVAILABILITY OF ABSTRACT
☐ UNCLASSIFIED/UNLIMITED ☐ SAME AS RPT. ☐ DTIC USERS

21. ABSTRACT SECURITY CLASSIFICATION
Unclassified

22a. NAME OF RESPONSIBLE INDIVIDUAL

22b. TELEPHONE (Include Area Code)

22c. OFFICE SYMBOL

DD FORM 1473, 84 MAR

83 APR edition may be used until exhausted.
All other editions are obsolete.

SECURITY CLASSIFICATION OF THIS PAGE
UNCLASSIFIED

The vibrationally mediated photodissociation dynamics of nitric acid

Amitabha Sinha, Randall L. Vander Wal, and F. Fleming Crim
Department of Chemistry, University of Wisconsin-Madison, Madison, Wisconsin 53706

(Received 9 February 1989; accepted 25 May 1989)

Vibrationally mediated photodissociation, in which one photon prepares a highly vibrationally excited molecule by vibrational overtone excitation and a second photon dissociates the vibrationally excited molecule, is a means of studying the spectroscopy and photodissociation dynamics of highly vibrationally excited states. Applying this dissociation scheme to nitric acid ($HONO_2$) excited in the region of the third overtone of the O–H stretching vibration ($4\nu_{OH}$) and detecting the OH fragment by laser induced fluorescence determines the energy partitioning and identifies the influence of vibrational excitation prior to dissociation. Vibrationally mediated photodissociation using 755 and 355 nm photons deposits *more* energy in relative translation than the isoenergetic single photon dissociation with 241 nm light. The former process also produces three times more vibrationally excited OH fragments, and both processes form electronically excited NO_2, which receives over three-quarters of the available energy. In these experiments, vibrational overtone excitation enhances the cross section for the electronic transition by about three orders of magnitude. The observed differences are consistent with the motion of the vibrationally excited molecule on the ground electronic state surface strongly influencing the dissociation dynamics by allowing access to different electronic states in the photolysis step.

I. INTRODUCTION

Photofragment spectroscopy provides a great deal of insight into the dynamics of molecular photodissociation.[1] Most studies investigate photodissociation from ground vibrational states, although there are examples involving vibrationally excited systems.[2,3] Because vibrational excitation gives a molecule access to regions of the ground electronic state potential energy surface that are unavailable to a vibrationless molecule, it may alter several aspects of the absorption of a second photon. Electronic excitation of a vibrationally excited molecule reaches otherwise inaccessible regions of the excited electronic potential energy surface by virtue of the vibrational motion on the lower surface. The change in initial geometry from that of the vibrationless molecule can potentially shift the absorption spectrum, alter the magnitude of the absorption cross section, and change the product quantum yield. Vibrational excitation can also induce vibronically allowed transitions that are unobservable from the ground vibrational state.[4]

We have recently implemented an approach that studies the effect of vibrational excitation on the photodissociation dynamics of molecules having stretches, such as those of C–H, O–H, and N–H bonds, that involve light atoms.[5] In these vibrationally mediated photodissociation experiments, one photon excites a vibrational overtone transition and a second photon, of a different wavelength, promotes the vibrationally energized molecule to a dissociative electronic state. Figure 1 illustrates this two-step process with schematic potential energy surfaces for a HOX molecule. In the ideal vibrationally mediated photodissociation experiment, neither photon is sufficiently energetic to dissociate the molecule from its vibrational ground state, and the combined energy of the two photons is less than that required to reach the electronically excited surface from the equilibrium geometry of the ground electronic state. As a result, dissociation by the second photon only occurs from geometries that are significantly different from the equilibrium configuration. Photodissociation through a bound vibrational overtone state is a means of studying the spectroscopy of highly vibrationally excited molecules. Because the OH fragment yield in these two-step photodissociation experiments depends on the first photon (λ_1) being resonant with a vibrational overtone transition, variation of its wavelength provides a vibrational overtone excitation spectrum. These spectra are complementary to laser photoacoustic spectra, and the two-photon technique has the added flexibility of being applicable to jet cooled samples.[6]

Here we describe the application of this two-color vibrationally mediated photodissociation scheme to nitric acid ($HONO_2$) using the third overtone of the O–H stretching vibration ($4\nu_{OH}$) to deposit the initial energy and using a second photon at $\lambda_2 = 355$ nm to dissociate the molecule. A third photon from another laser monitors the dissociation process by laser-induced fluorescence on the $A \leftarrow X$ transition of the OH photofragment. For purposes of comparison, we dissociate $HONO_2$ with a single photon at 241 nm, a wavelength that corresponds to the same total added energy as in the two-color vibrationally mediated photodissociation. The distribution of products among their rovibrational states, as determined by laser induced fluorescence, and the extent of translational energy disposal, as inferred from the Doppler widths in the laser induced fluorescence spectra, reflect the differences between the photodissociation dynamics through a highly vibrationally excited intermediate state and those for direct single photon dissociation at a comparable total energy.

Nitric acid is a particularly attractive candidate for vibrationally mediated photodissociation measurements. The O–H stretching vibration is a means of energizing the molecule vibrationally, and relatively low lying excited states allow photodissociation at convenient wavelengths. Figure 2 shows the near ultraviolet absorption spectrum of $HONO_2$ taken from the work of Biaume.[7(a)] It is rather structureless

 0021-9606/89/172929-10$02.10

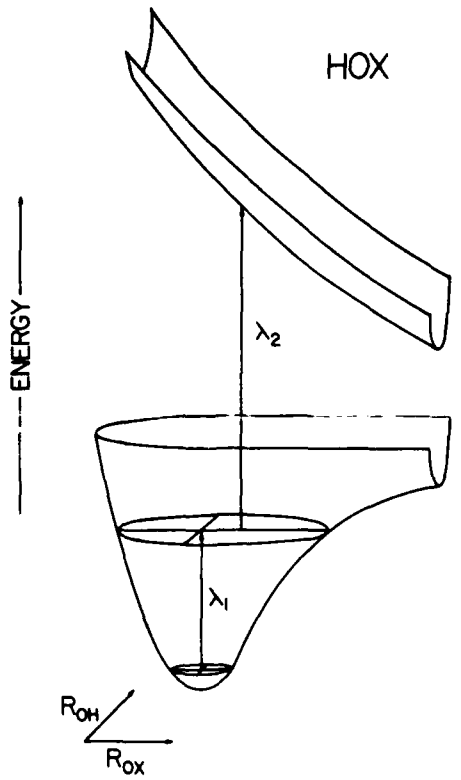

FIG. 1. Schematic drawing of bound and dissociative potential energy surfaces illustrating vibrationally mediated photodissociation. The lower surface is bound in both the OH and OX stretching coordinates, and the upper surface is dissociative in the latter. The vibrational overtone excitation wavelength is λ_1 and the photolysis wavelength is λ_2. We omit the coordinates for the internal degrees of freedom of X from this simplified picture and fix the bending coordinate of HOX, which could play a role in the dissociation dynamics, for this cut through the potential energy hypersurface. In the present experiments, X is NO_2.

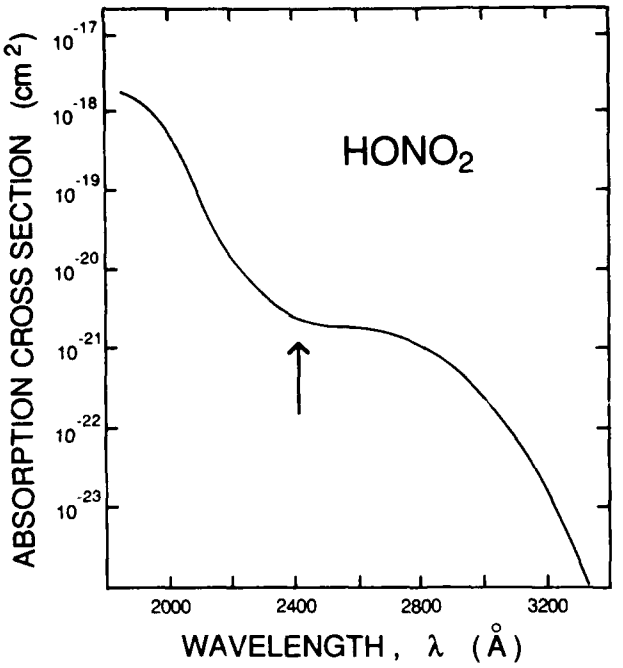

FIG. 2. Ultraviolet absorption spectrum redrawn from the work of Biaume (Ref. 7). The arrow indicates the wavelength of single photon excitation that adds the same amount of energy as vibrationally mediated photodissociation.

with two prominent maxima suggesting transitions to several electronic states. Complete neglect of differential overlap/configuration interaction (CNDO/s-CI) calculations by Harris[8] indicate that three singlet electronic surfaces dominate the photochemistry of nitric acid in this wavelength region. He has assigned the band system centered around 270 nm to an electronic state of $^1A''$ symmetry ($^1A'' \leftarrow {}^1A'$) and attributed the more intense feature at 185 nm to transitions to a $^1A'$ state.[8] The calculations also find a second $^1A''$ state whose contribution to the absorption spectrum may be hidden under the more intense $^1A' \leftarrow {}^1A'$ transitions. All three electronic transitions involve excitation to a π^* antibonding orbital primarily localized on the NO_2 chromophore.

There have been several studies of the photodissociation of $HONO_2$ from its vibrational ground state.[9-11] The most detailed of these, by August *et al.*,[10] uses 280 nm photons and measures both scalar and vector properties of the OH photofragment. They conclude that the $^1A'' \leftarrow {}^1A'$ transition at 280 nm is a vibronic transition induced by ONO' out-of-plane vibrational motion and that nitric acid undergoes a change in geometry from being planar in its ground electronic state to being pyramidal in the first excited singlet state in accord with Walsh's rules. Less is known about the band system of $HONO_2$ at 185 nm. Jacobs *et al.*[11] find that most of the excess energy in the 193 nm photolysis goes into relative translation of the fragments and internal excitation of the NO_2 group. The products preferentially populate the lower lambda doublet component $\{P[\Pi(A')]/P[\Pi(A'')] = 2.6\}$, which is opposite to the trend observed by August *et al.*[10] in the 280 nm photolysis.[12] The change in the lambda doublet state populations shows that the dissociation dynamics on the surfaces accessible at 193 nm are different from those at 280 nm.

Our vibrationally mediated photodissociation experiments use 755 nm light for exciting the $4\nu_{OH}$ transition and 355 nm light for the dissociation, a choice dictated partly by experimental convenience and partly by our expectation that vibrational excitation shifts the absorption spectrum (Fig. 2) to longer wavelengths. Thus, adding the energy of a 241 nm photon, which approximately corresponds to the midpoint between the two absorption maxima, potentially allows us to access different electronic surfaces depending on whether the excitation occurs by a two-step vibrationally mediated process or a single-step process of equivalent energy. Because excitations into the two absorption bands produce different dissociation dynamics, we anticipate corresponding differences in the single photon and vibrationally mediated processes.

II. EXPERIMENTAL APPROACH

The apparatus shown in Fig. 3 is a modified version of the one used in studies of vibrational overtone induced predissociation.[13] In our room temperature, vibrationally mediated photodissociation measurements, we combine ~30 mJ

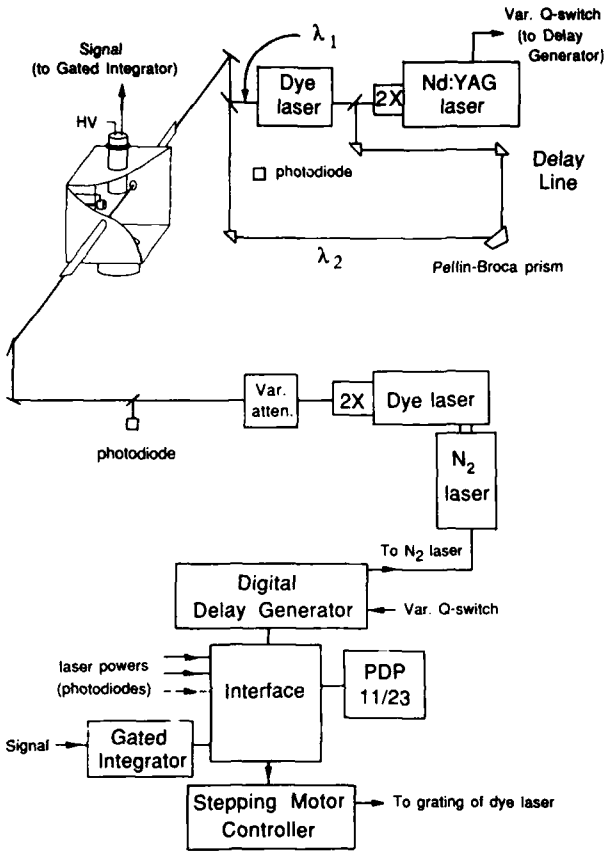

FIG. 3. Schematic diagram of the experimental apparatus.

pulses of light from a Nd:YAG laser pumped dye laser (the vibrational overtone excitation laser) in the region of 755 nm and 3–5 mJ pulses of 355 nm light from the third harmonic of the Nd:YAG laser (the photolysis laser) on a dichroic mirror and send them into a vacuum chamber through which 60–75 mTorr of anhydrous nitric acid continuously flows. Two independent lens systems, located before the dichroic mirror, collimate and reduce the vibrational overtone excitation and photolysis laser beams such that their diameters in the detection region are approximately 2 and 3 mm, respectively. Optically delaying the photolysis light (λ_2), which is generated prior to that for vibrational overtone excitation (λ_1), ensures the temporal coincidence of the two pulses. Frequency-doubled light around 308 nm from a nitrogen laser pumped dye laser (the probe laser) counterpropagates relative to the other two laser beams with a typical delay between the probe laser and the photolysis laser pulse of 50 ns. A photomultiplier (EMI 9635QB) views the OH fluorescence excited by the probe laser through an $f/2$ optical system, and a gated integrator captures the resulting signal. A laboratory computer accumulates the fluorescence signal along with those from photodiodes that monitor the energy of each laser pulse. Two dichroic edge filters having a sharp cutoff at 355 nm, a colored glass filter (Corning 7-54), and baffles in the sidearms leading into the chamber reduce scattered light from the photolysis pulse.

Light for the 241 nm single photon photolysis comes from a second Nd:YAG/dye-laser system (Quanta-Ray DCR-2A/PDL-2/WEX-1). We generate 241 nm radiation by mixing the frequency doubled light from the dye laser, in the region of 320 nm, with the 1.06 μm fundamental of the Nd:YAG laser. In order to minimize contributions from two-photon photodissociation of nitric acid, which appears to be quite efficient at this wavelength,[14] we keep the pulse energy below 0.2 mJ and the beam diameter in the interaction region relatively large ($\sim$4 mm).

We record room temperature photoacoustic spectra in the region of the third overtone of the O–H stretching motion ($4\nu_{OH}$) using a microphone attached to a cell containing 7–10 Torr of anhydrous nitric acid. A 0.025 mm thick stainless steel diaphragm isolates the microphone (Knowles BT-1751) from the corrosive sample. After laser excitation of the gas, collisional transfer of energy from internal to translational degrees-of-freedom produces an acoustic wave that the diaphragm transmits to the microphone. We prepare anhydrous nitric acid by bubbling a stream of nitrogen through a mixture containing three parts sulfuric acid and one part nitric acid and collecting the anhydrous nitric acid, which is entrained in the nitrogen flow, in a flask cooled to dry ice temperature. The nitric acid sample is stored at -20 °C and thoroughly degassed before use. Because anhydrous nitric acid is very corrosive, the sample introduction system is all glass and Teflon.

III. RESULTS

A. Vibrational overtone excitation spectra

The thermodynamic threshold energy for production of ground state OH and NO_2 fragments from nitric acid is 16 700 cm^{-1},[15] and, thus, exciting the third overtone of the O–H stretching vibration ($4\nu_{OH}$) at 13 250 cm^{-1} supplies too little energy to dissociate the molecule. However, additional energy provided by the second (photolysis) photon dissociates the molecule by exciting it to a repulsive excited electronic state, as illustrated schematically in Fig. 1. Scanning the vibrational overtone excitation laser wavelength (λ_1) while monitoring a particular quantum state of the OH fragment maps out the vibrational overtone excitation spectrum of bound levels from which the second photon (λ_2) dissociates the molecule to form a fragment in the interrogated quantum state.

The vibrational overtone excitation spectrum of the $4\nu_{OH}$ transition shown in Fig. 4(a) comes from monitoring the total fluorescence excited from the $Q_1(4)$ rotational line of the OH($A\,^2\Sigma^+, v' = 0 \leftarrow X\,^2\Pi, v'' = 0$) transition while scanning the wavelength of the vibrational overtone excitation laser in the region of 755 nm. Vibrational overtone excitation spectra generated by monitoring other OH transitions are identical to the one shown. The dependence of the OH laser induced fluorescence intensity on the power levels of both the vibrational overtone excitation and the photodissociation lasers, shown in Fig. 5, confirms that we are observing a two-photon (1 + 1) vibrationally mediated photodissociation process that is linear in both the vibrational overtone and photolysis laser pulse energies. The observed position of the band center in the vibrational overtone excitation spectrum agrees well with predictions of a simple local mode model. The Birge–Sponer plot for nitric acid in Fig. 6

A-1,20

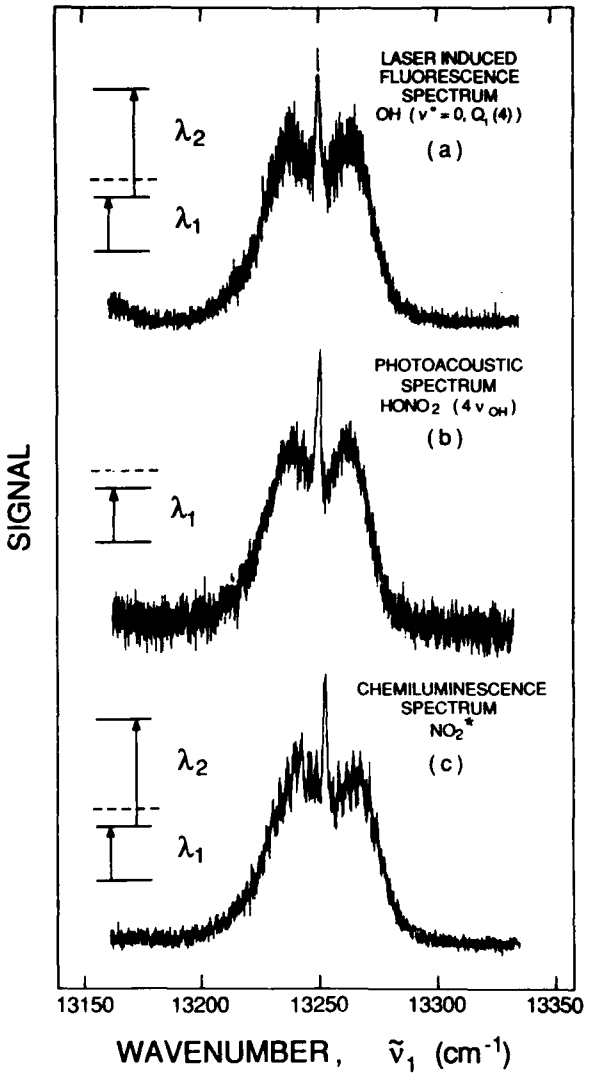

FIG. 4. Vibrational overtone spectra of $HONO_2$ in the region of the third vibrational overtone transition ($4\nu_{OH}$). (a) Vibrational overtone excitation spectrum detecting $OH(v''=0)$ on the $Q_1(4)$ line of the $A \leftarrow X$ transition. (b) The photoacoustic absorption spectrum in a 10 Torr sample. (c) The vibrational overtone excitation spectrum detecting chemiluminescence from the electronically excited NO_2 product.

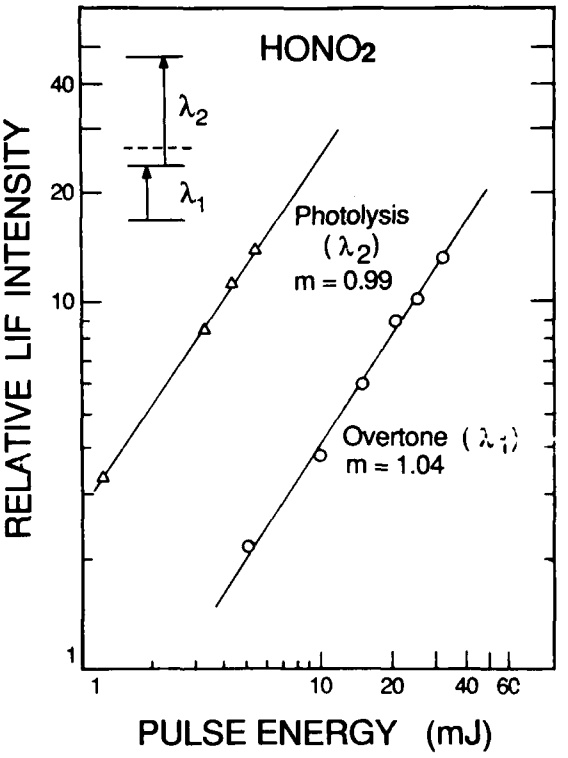

FIG. 5. Variation of the laser induced fluorescence signal intensity with the energy of the vibrational overtone excitation laser pulse (λ_1) and the photolysis pulse (λ_2).

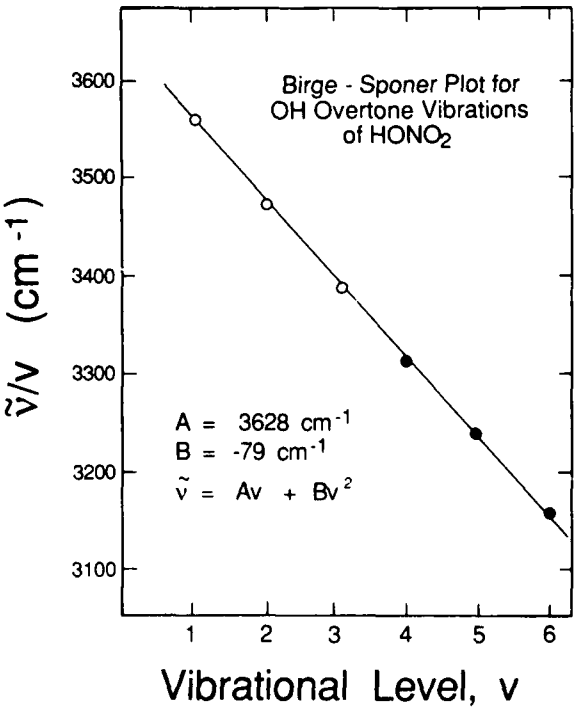

FIG. 6. Birge–Sponer plot for the O–H stretching transitions in nitric acid. The solid points are from photoacoustic spectroscopy, vibrationally mediated photodissociation, and vibrational predissociation, and the open points are from infrared and near infrared absorption measurements (Ref. 17). The transition wave numbers obey the relation $\tilde{\nu} = Av + Bv^2$ where $\omega_e = A - B$ is the mechanical frequency and $\omega_e x_e = -B$ is the anharmonicity.

shows that the O–H stretching vibrations in the molecule follow the anharmonic oscillator behavior that is characteristic of local mode vibrations.[16] The open points in the plot are from earlier infrared and near infrared measurements,[17] and the solid points come from our vibrationally mediated photodissociation and vibrational overtone predissociation studies.[18]

The spectrum in Fig. 4 has an inhomogeneous width of 50 cm^{-1} that arises primarily from rotational congestion in the room temperature sample. The distinct *P*-, *Q*-, and *R*-branch structure in the spectrum suggests that the vibrational overtone transition is a hybrid band involving *a*- and *b*-type transitions,[19] and preliminary spectral simulations confirm this analysis. The hybrid nature of this band is consistent with microwave measurements[20] that find the O–H bond angle with the *a* axis is ~62°. The bond-dipole approxi-

mation,[16] which places the transition moment for the vibrational overtone excitation along the O–H stretching coordinate, predicts both *a* and *b* components in the spectrum. In contrast to the situation for hydrogen peroxide,[5(b)] spectral features involving the torsional modes are not present, an observation which suggests that the coupling between torsional modes and the O–H stretching coordinate in nitric acid is weak. Figure 4 also shows a room temperature photoacoustic spectrum of nitric acid in the region of the third overtone vibration ($4\nu_{OH}$) that is identical to the one obtained by vibrationally mediated photodissociation. The photoacoustic spectrum is sensitive to states having significant O–H stretching character[16] while the two-step vibrationally mediated process depends on states having not only O–H character but also a good Franck–Condon with the excited electronic state. The similarity of the two spectra suggests that all rovibrational states lying under the vibrational overtone band have roughly similar Franck–Condon factors and that spectral congestion obscures any subtle differences.

B. Product state distributions

Excitation via either a single photon or a vibrationally mediated process provides nitric acid with $\sim 25\,000\ cm^{-1}$ of excess energy for distribution among the fragments, and the laser induced fluorescence excitation spectrum of the OH photofragment reveals the allocation of this energy among the various degrees of freedom. Figure 7 shows the rotational state distribution for the $OH(X\,^2\Pi_{3/2}, v'' = 0)$ fragment. The open symbols are for the single photon process, and the solid ones are for vibrationally mediated photodissociation with the wavelength of the vibrational overtone laser (λ_1) fixed at the central maximum of the excitation spectrum. The rotational distributions for the two processes are identical within the experimental uncertainties. Both rotational distributions, which have maxima around $N'' = 4$, extend up to $N'' = 14$ and approximately follow a Boltzmann distribution with a temperature of (1550 ± 100) K. The majority of the OH photofragments appear in $v'' = 0$ in both the one- and two-photon experiments, and the vibrationally mediated process produces significantly more (6% compared to 2%) vibrationally excited OH fragments. Because of the low population in the $OH(^2\Pi, v'' = 1)$ level, we are unable to determine the nascent rotational state distribution within this vibrational state; however, by using relatively high $HONO_2$ pressures (0.5 Torr), we are able to obtain a nascent *vibrational* distribution, since for polar diatomic molecules vibrational relaxation is much slower than rotational relaxation.[21] We also extract the translational energy release from the linewidth in the laser induced fluorescence excitation spectrum, as shown in Fig. 8. For the vibrationally mediated process, a laser-linewidth-deconvoluted[22] Doppler width of $\Delta\tilde{\nu}_D = (0.47 \pm 0.03)\ cm^{-1}$ (FWHM) for the $Q_1(4)$ transition shows that $\sim 20\%$ of the available energy goes into relative translation of the fragments. The single photon photolysis at 241 nm produces a narrower line, $\Delta\tilde{\nu}_D = (0.35 \pm 0.03)\ cm^{-1}$, that reflects the deposition of less

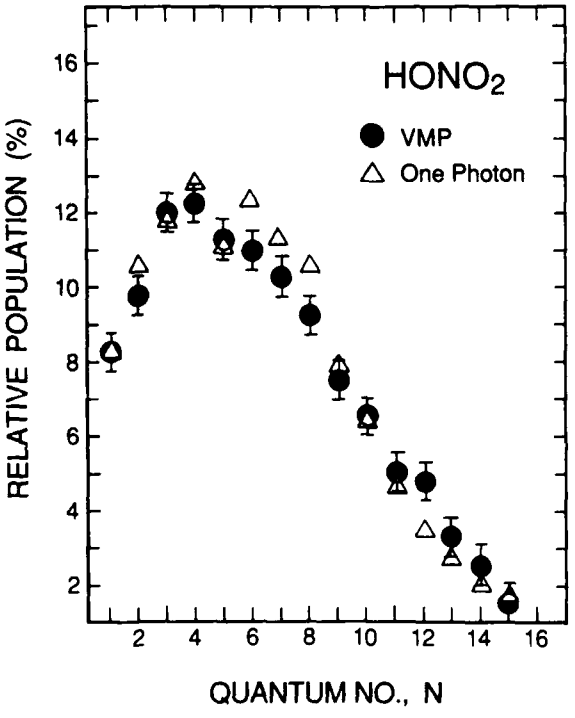

FIG. 7. Relative population of product rotational states for the vibrationally mediated photodissociation (closed circles) and single photon dissociation (open triangles) of nitric acid. The quantum number N corresponds to the total angular momentum except for electron spin.

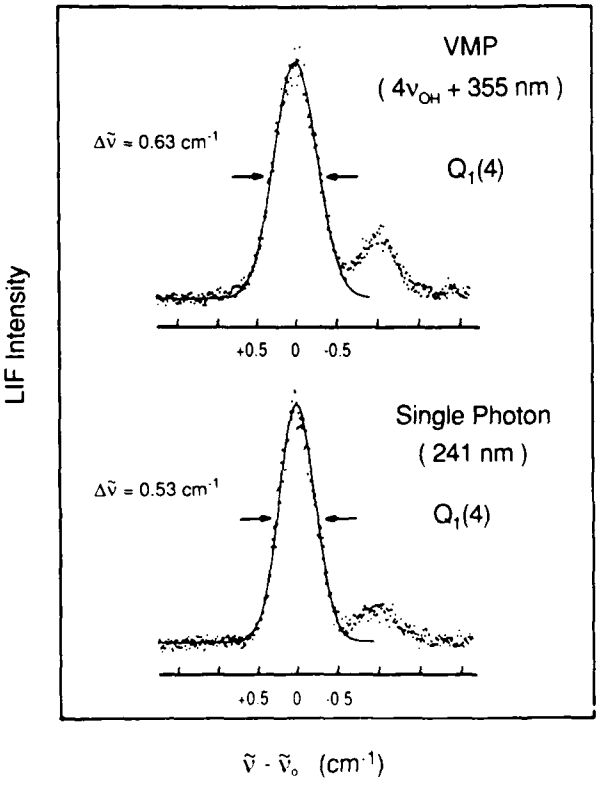

FIG. 8. Doppler profile for the OH $Q_1(4)$ transition resulting from vibrationally mediated photodissociation and isoenergetic single photon dissociation. The linewidth of the ultraviolet probe laser is 0.4 cm^{-1}. The smooth line through the points is a Gaussian curve having the indicated width $\Delta\tilde{\nu}$.

TABLE I. Energy disposal in the vibrationally mediated and single photon dissociation of nitric acid.[a]

	Vibrationally mediated photodissociation	241 nm photolysis	280 nm[b] photolysis
E_{avail}[c]	25 190	25 190	19 470
E_T(OH)	3 423	1 898	4 090
	(0.136)[d]	(0.075)	(0.21)
E_R(OH)	1 000	1 000	890
	(0.04)	(0.04)	(0.046)
E_V(OH)	200	56	< 390
	(0.008)	(0.002)	(< 0.02)
$E_T(NO_2)$[e]	1 265	702	1 510
	(0.05)	(0.028)	(0.078)
$E_{int}(NO_2)$[e]	19 298	21 537	12 596
	(0.766)	(0.855)	(0.646)

[a]Units of cm^{-1}.
[b]Reference 10.
[c]The available energy is the photon energy and average initial thermal energy less the bond dissociation enthalpy $E_{avail} = h\nu + E_{thermal} - \Delta H_0^0$.
[d]The quantity in parenthesis is the fraction of the available energy in that degree of freedom.
[e]The NO_2 translational energy is inferred from momentum conservation in conjunction with measured Doppler width of the OH fragment. The NO_2 internal excitation is inferred from energy conservation.

energy into relative translation. Table I summarizes the results of these energy disposal measurements.

We infer from energy conservation that over three-quarters of the available energy must reside in internal excitation of the NO_2 fragment in both dissocation processes. The presence of low lying excited electronic states of NO_2, such as the $1\ ^2B_1$ and $1\ ^2B_2$ states,[23,34] makes it improbable that this fraction, which corresponds to over 19 000 cm^{-1} of energy, goes solely into vibration and rotation of the NO_2. Indeed, we observe visible chemiluminescence in both the vibrationally mediated and single photon photodissociations. This chemiluminescence, which we observe through a filter arrangement having an effective bandpass of 480–580 nm, has a radiative lifetime of $\sim 3\ \mu s$ at a pressure of 80 mTorr. The fluorescence characteristics of possible emitters (OH, NO_2, and $HONO_2$) lead us to assign the observed emission to electronically excited NO_2,[15] although we do not yet know the symmetry of the emitting state(s). Figure 4(c) shows a vibrational overtone excitation spectrum of the $4\nu_{OH}$ band obtained by monitoring this NO_2 photofragment emission. These data, like those in Fig. 4(a), come from scanning the vibrational overtone excitation laser (λ_1) in the region of the $4\nu_{OH}$ transition while fixing the photolysis laser (λ_2) at 355 nm, but in this case we monitor the chemiluminescence from electronically excited NO_2. The similarity of this spectrum to those in Figs. 4(a) and 4(b), as well as measurements that show the NO_2 emission intensity to be linear in both the vibrational overtone excitation (λ_1) and photolysis (λ_2) laser energies, confirms that electronically excited NO_2 comes directly from the photodissociation.

Relative populations of the lambda doublet components are another probe of the dissociation process. We use the nomenclature recently proposed by Alexander *et al.*[24] to denote the two lambda doublet components as either $\Pi(A')$ or $\Pi(A'')$ depending on whether the electronic wave function is symmetric or antisymmetric for reflection in the plane of rotation. For the OH radical in the limit of high J, the $\Pi(A')$ states have the orbital containing the unpaired electron in the plane of rotation of the fragment while the $\Pi(A'')$ states have this orbital perpendicular to the plane. Figure 9 displays the ratio of populations P in the lambda doublet states for rotational levels ranging from $N'' = 2$ to $N'' = 10$, as obtained by monitoring the $Q_1(N)$ and $P_1(N)$ branches in $OH(^2\Pi_{3/2})$. The results clearly show a measurable difference in the population ratio, $P[\Pi(A')]/P[\Pi(A'')]$, for the single photon and vibrationally mediated photodissociations. Because the relative intensities of the Q- and P-branch transitions are also affected by fragment alignment,[25] we vary the relative polarization of the photolysis and probe beams as a test.[26] The very slight sensitivity of the population ratios to variations in the relative polarization of the probe and photolysis lasers shown in the two panels of Fig. 9 indicates that there is negligible fragment alignment. We can also monitor the population of the two electronic fine structure components in the OH product. The population of the lower energy $^2\Pi_{3/2}$ spin–orbit state is slightly larger (1.1 ± 0.15) in both the single photon and vibrationally mediated photodissociations.

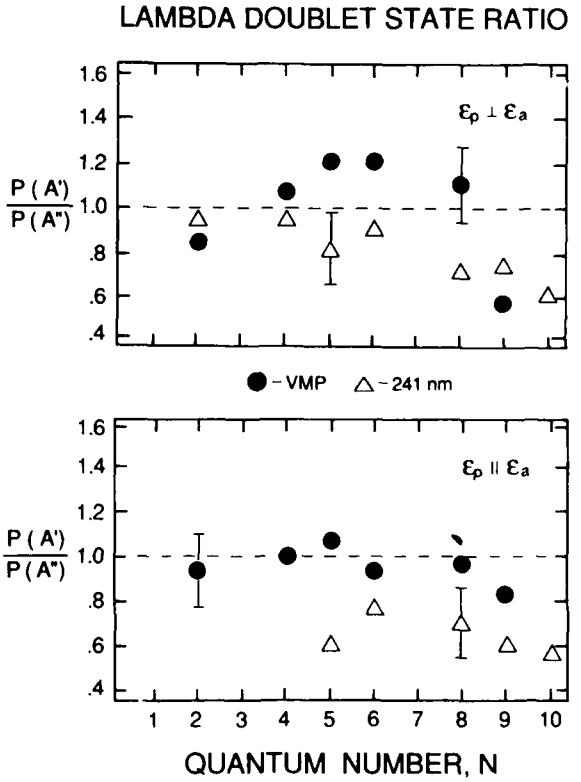

FIG. 9. Ratio of the populations in the lambda doublet states in the vibrationally mediated photodissociation (closed circles) and single photon dissociation (open triangles) of nitric acid for two different relative polarizations of the photolysis and probe lasers. In the upper panel, the polarizations of the photolysis and probe lasers are perpendicular to each other and in the lower panel they are parallel. In the vibrationally mediated photodissociation, the vibrational overtone excitation laser and photolysis laser have the same polarization.

C. Absorption cross section

Vibrational overtone transitions have inherently low excitation probabilities. For example, the cross section for exciting the third overtone of the O–H stretching motion ($4\nu_{OH}$) is about $\sim 1\times10^{-23}$ cm^2.[27] Obtaining adequate signals in our two-step vibrationally mediated photodissociation experiments relies on the tremendous increase, also observed by other investigators,[2] in the electronic absorption cross section upon vibrational excitation. This increase appears to compensate partly for the low efficiency of vibrational overtone excitation. We are able to estimate the electronic absorption cross section from the $4\nu_{OH}$ level of nitric acid by comparing the relative yield of OH photofragments in the single- and two-photon processes. Applying Beer's law to the absorption and using known values for the single photon ultraviolet absorption cross section,[7,28,29] we calculate the absorption cross section out of the $4\nu_{OH}$ level to be $\sim 1\times10^{-17}$ cm^2,[30] as described in the Appendix. Comparing this value with that for single-photon dissociation at 241 nm, $\sigma(241) = 2.5\times10^{-20}$ cm^2, shows that vibrational overtone excitation enhances the absorption cross section of nitric acid by roughly three orders of magnitude.[31]

IV. DISCUSSION

The results described above and summarized in Table I show that two-step vibrationally mediated photodissociation of nitric acid has very different dynamics than the one-photon ultraviolet dissociation at comparable energy. The differences are apparent in the translational energy release, vibrational state populations, lambda double state ratios, and absorption cross sections, but the lack of detailed *ab initio* calculations hampers the interpretation of these differences in terms of excited state potential energy surfaces. The CNDO/s-CI calculation of Harris assigns the main features in the near ultraviolet absorption spectrum of nitric acid to $\pi^*\leftarrow n_0$, $\pi^*\leftarrow\sigma$, and $\pi^*\leftarrow\pi$ transitions[8] but does not provide any information about the changes in the excited state potential energy surfaces along the various vibrational coordinates or about the product states to which these surfaces correlate. In the absence of more detailed published calculations, we use a correlation diagram and the preliminary results of a more accurate *ab initio* calculation by Bai and Segal[32] to understand several aspects of the vibrationally mediated photodissociation of nitric acid.

A. Electronic states and correlation diagram

The orbital correlation diagram in Fig. 10, which is the result of calculations by Glendening and Weinhold,[33] shows the valence molecular orbitals of $HONO_2$ on the left-hand side and those of the NO_2 and OH fragments on the right-hand side, in order of increasing energy. (We only consider dissociation channels that produce OH and NO_2 fragments since OH quantum yield measurements[29] indicate that these two species dominate for wavelengths longer than 200 nm.) The $3a''$ molecular orbital is the highest one occupied in the ground electronic state of nitric acid, and the corresponding highest occupied orbitals in the NO_2 and OH fragments in their ground electronic states are $6a_1$ and π, respectively.

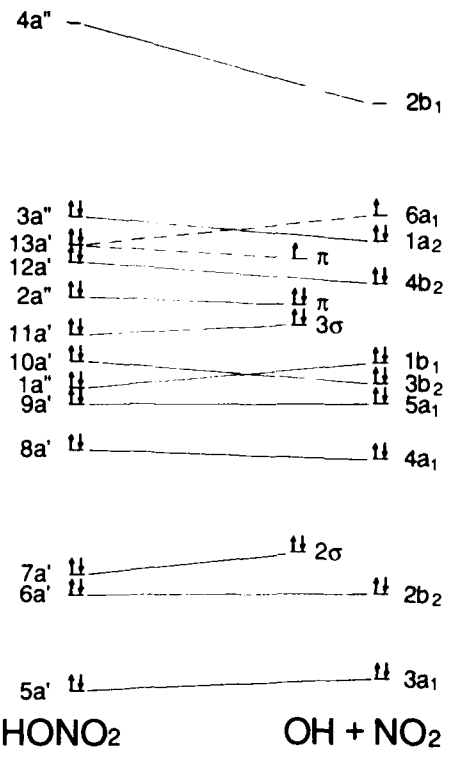

FIG. 10. Orbital correlation diagram between $HONO_2$ and the dissociation products OH and NO_2.

The $13a'$ orbital in nitric acid is primarily responsible for bonding between the OH and NO_2 moieties and correlates to both an OH molecular orbital (π) and an NO_2 orbital ($6a_1$) when ground electronic state $HONO_2$ separates into its fragments, as shown by the two dashed lines in Fig. 10. We classify all the other molecular orbitals of the $HONO_2$ molecule as having primarily NO_2 or OH character and correlate them to single product orbitals.

According to Harris,[8] the $\pi^*\leftarrow n_0$, $\pi^*\leftarrow\sigma$, and $\pi^*\leftarrow\pi$ transitions in nitric acid correspond to removing an electron from the $12a'$, $13a'$, or $3a''$ orbital, respectively, and promoting it to the $4a''$ orbital. The correlation diagram gives the configuration for each excitation and allows us to identify, in the context of this simple picture, the possible NO_2 fragment electronic states. Using extensive *ab initio* calculations by Jackels and Davidson,[34] we identify the configurations and corresponding states of NO_2 that correlate diabatically with different excited states of $HONO_2$ as

$$\pi^*\leftarrow n_0 \quad \cdots(4b_2)^1(1a_2)^2(6a_1)^1(2b_1)^1, \quad NO_2(2\,^2A_2),$$

$$\pi^*\leftarrow\sigma \quad \cdots(4b_2)^2(1a_2)^2(6a_1)^0(2b_1)^1, \quad NO_2(1\,^2B_1),$$

$$\pi^*\leftarrow\pi \quad \cdots(4b_2)^2(1a_2)^1(6a_1)^1(2b_1)^1, \quad NO_2(2\,^2B_2).$$

These correlations show that dissociation of $HONO_2$ from its electronically excited states is likely to produce electronically excited fragments, in agreement with our observation of chemiluminescence in both single photon and vibrationally mediated photodissociation. These diabatic correlations, which do not include avoided crossings with high lying states of $HONO_2$ that correlate to low lying states of NO_2, are only a limiting case, and we must also consider the adia-

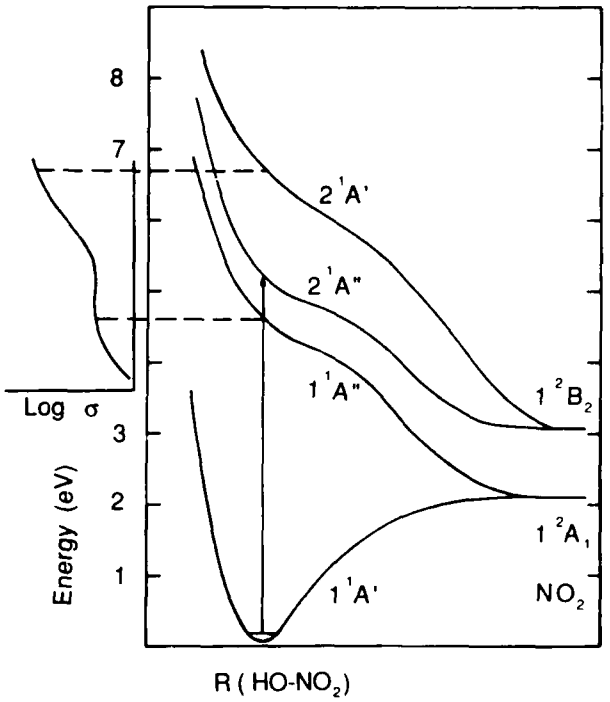

FIG. 11. Potential energy curves for the dissociation of nitric acid to OH and NO_2 (adapted from the calculations of Bai and Segal, Ref. 32).

batic curves, which would result from the crossings being strongly avoided, to obtain a complete picture of the dissociation dynamics. Figure 11 shows completely adiabatic potential energy curves, adapted from the recent *ab initio* calculations of Bai and Segal,[32] in which all the crossings are avoided. If the dissociation proceeds adiabatically, excitation of the $1\,^1A''$ state of nitric acid produces ground electronic state NO_2 and excitation of the $2\,^1A''$ state produces electronically excited NO_2 in its $1\,^2B_2$ state. The bond angles and lengths in ground electronic state NO_2 closely resemble those in ground electronic state $HONO_2$, but the electronically excited states of NO_2, to which many excited states of $HONO_2$ correlate, have rather different bond angles. This large geometry change should produce significant vibrational excitation accompanying the electronic excitation of the NO_2 product from the ultraviolet dissociation of $HONO_2$.

B. Single photon ultraviolet photodissociation

Single photon dissociation experiments are an important point of comparison with vibrationally mediated photodissociation, and the photodissociation experiments on nitric acid at 280 nm by August *et al.*,[10] which include vector correlation measurements, are especially useful in this regard. As Table I shows, the higher energy 241 nm dissociation deposits a fraction of the total energy in fragment translation that is almost three times *less* than that in the 280 nm photolysis. This observation suggests that these single photon excitations access different excited electronic states that produce the observed differences in the energy partitioning. The potential energy curves in Fig. 11 suggest that the 241 nm excitation, denoted by the vertical arrow, predominantly reaches the $2\,^1A''$ electronic state while the 280 nm excitation accesses the lower energy $1\,^1A''$ surface. The smaller translational energy release in the 241 nm photolysis compared to the 280 nm dissociation is consistent with excitation to the $2\,^1A''$ state, since the correlation of the $2\,^1A''$ state to a higher energy electronic state of the NO_2 product would produce correspondingly less energy in translation for the 241 nm excitation. Both the 241 nm and the 280 nm[10] single photon dissociations produce a preferential population of the $\Pi(A'')$ lambda doublet component for high J states of the OH fragment. August *et al.*[10] suggest that torsional motion in the excited state is an essential feature of the dissociation dynamics of $HONO_2$. They conclude that the nodal structure of the π^* antibonding orbital excited in the $\pi^* \leftarrow n_0$ transition at 280 nm produces this torsion, and we expect similar behavior when populating the same π^* orbital in a $\pi^* \leftarrow \sigma$ transition at 241 nm.

C. Vibrationally mediated photodissociation

The crucial difference between vibrationally mediated and single-photon phtodissociation is the larger range of nuclear configurations available in the former. This allows different electronic surfaces to participate in the dissociation and to produce the observed differences in translational energy release and lambda doublet state populations for the isoenergetic single-photon and vibrationally mediated photodissociations. Transitions from the vibrationally excited intermediate state to the dissociative electronic state occurring from the compressed HO–N bond at the inner turning point may well reach the $1\,^1A''$ state rather than the higher energy $2\,^1A''$ state that seems to participate in the one-photon 241 nm dissociation. Since the $1\,^1A''$ surface adiabatically correlates with a lower energy fragment [$NO_2(X\,^2A_1)$] than the $2\,^1A''$ surface, more energy is available for translation, as observed in the Doppler profiles and reported in Table I for the vibrationally mediated and single photon processes. Transitions from the extended HO–N bond near the outer turning point potentially reach the $2\,^1A''$ electronically excited state to produce electronically excited fragments, whose emission we observe in the vibrationally mediated process. Thus, transitions from geometries that are accessible only through the vibrationally excited intermediate state explain the larger average translational energy release that we observe in vibrationally mediated photodissociation compared to single photon dissociation as well as the production of electronically excited NO_2 fragments. However, in the absence of more quantitative information about the surfaces and Franck–Condon factors, we are unable to assess the relative contribution of transitions from the two turning points.

Both two-step vibrationally mediated photodissociation and single photon dissociation produce mostly vibrationally unexcited OH fragments, but the vibrational state distributions are quite different for the two processes. The vibrationally mediated photodissociation produces almost three times as many OH molecules in $v'' = 1$ as the isoenergetic single photon dissociation even though the fractions, 6% and 2%, respectively, are small in both cases. We have found even larger population enhancements in the vibrationally mediated photodissociation of hydrogen peroxide.[5] It appears that

the O–H stretching character of the intermediate state, which is essential for vibrational overtone excitation, partially survives in the two-step photodissociation.

The three orders of magnitude enhancement in the dissociation cross section for vibrationally excited molecules is perhaps the most dramatic indicator of the differences vibrationally mediated and single photon dissociation. This enhancement could arise from improved Franck–Condon factors for the vibrationally excited molecule or from coupling of $^1A''$ electronic states with states of $^1A'$ electronic symmetry, to which there are strong transitions from the ground state. August *et al.*[10] invoke this vibronic coupling mechanism to explain their 280 nm photodissociation measurements. Experiments that measure the anisotropy parameter β for the single photon and vibrationally mediated processes,[35] should allow us to differentiate between the two possible mechanisms responsible for enhancing the absorption cross section by determining the orientation of the transition moment in the photodissociations.

V. SUMMARY

Two-color vibrationally mediated photodissociation is a means of studying both the spectroscopy of bound vibrational states and the photodissociation dynamics of highly vibrationally excited molecules. It is particularly well suited to molecules having stretching vibrations involving light atoms and low lying, *dissociative* excited electronic states. We have used this scheme to study nitric acid molecules that are initially excited in the region of the third overtone of the O–H stretching vibration ($4\nu_{OH}$). Subsequent absorption of a 355 nm photon by the vibrationally energized molecule promotes it to a repulsive electronic state from which it dissociates to form OH and NO_2 fragments. We use laser induced fluorescence to detect individual quantum states of the OH fragments, and we infer the recoil energy from the linewidths in the laser induced fluorescence excitation spectra.

Comparing the energy disposal in the vibrationally mediated photodissociation with that in an isoenergetic single photon ultraviolet photodissociation reveals subtle differences that arise from the initial nuclear configurations sampled prior to electronic excitation. We suspect that direct single photon excitation at 241 nm, which primarily originates from the ground state equilibrium configuration, reaches the $2\,^1A''$ electronic state but that the isoenergetic vibrationally mediated process occurs from rather different geometries. Consideration of the potential energy surfaces involved suggest that the dissociation through the highly vibrationally excited state occurs from an initially compressed HO–N bond, producing transitions to the $1\,^1A''$ electronic surface, or from an extended HO–N bond, potentially reaching the $2\,^1A''$ electronic state. Without more details about the potential energy surfaces, it is difficult to establish the relative importance of these two contributions. Clearly vibrationally mediated photodissociation samples excited electronic states that are inaccessible in an isoenergetic direct single photon absorptions. Experiments that measure vector correlations in these two isoenergetic processes should provide greater insight into the dynamical differences and help identify the origin of the thousand-fold enhancement in the absorption cross section upon vibrational excitation.

ACKNOWLEDGMENTS

We thank Professor F. A. Weinhold and Professor R. W. Field for several helpful discussions and E. Glendening and Professor Weinhold for performing molecular orbital calculations on nitric acid. We appreciate Professor Segal's communicating the results of his *ab initio* calculations on nitric acid to us prior to their publication. We also thank Dr. M. D. Likar for help with the data acquisition programs and J. L. Scott for help with the figures. We gratefully acknowledge the support of this work by the Army Research Office.

APPENDIX

We estimate the cross section for photoabsorption out of the vibrational overtone excited state by comparing the relative OH fragment yield in the vibrationally mediated photodissociation experiment with that from single photon dissociation at 246 nm using Beer's law. In these cross section measurements, the diameters of the vibrational overtone excitation beam (λ_1) and the photolysis beam (λ_2) are matched in the interaction zone, and the diameter of the probe laser beam is always smaller than that of the photolysis and vibrational overtone excitation lasers. In the limit of small absorption, Beer's law is

$$\Delta N = N_0 \sigma \rho l , \tag{A1}$$

where ρ is the number density, N_0 is the number of incident photons, σ the cross section, and l the interaction length, respectively. The number of molecules excited by the vibrational overtone excitation laser (λ_1) and by the photolysis laser (λ_2) are

$$n_1 = N_{ovt} \sigma_{ovt} \rho_0 l , \tag{A2}$$

and

$$n_2 = N_{sss} \sigma^* \rho_1 l . \tag{A3}$$

By using $\rho_1 = n_1 / V_{ovt} = (N_{ovt} \sigma_{ovt} \rho_0 l / V_{ovt})$ in Eq. (A3) and noting that the beam diameters for the vibrational overtone excitation and photolysis lasers are the same over the interaction region, we obtain

$$n_2 = N_{sss} N_{ovt} \sigma^* \sigma_{ovt} \rho_0 (l^2 / V_{ovt}) , \tag{A4}$$

where V_{ovt} is the volume occupied by the vibrational overtone excitation beam in the interaction region. The laser induced flurorescence signal is proportional to the number of OH fragments produced (n_{OH}) which in turn is proportional to n_2, the number of electronically excited $HONO_2$ molecules generated. If we assume that every electronically excited $HONO_2$ produces an OH, then the signal for the vibrationally mediated photodissociation experiment, S_{vmp} is

$$S_{vmp} \propto N_{probe} \sigma_{OH} \rho_{OH} l = N_{probe} \sigma_{OH} (n_2 / V_{ovt}) l . \tag{A5}$$

Substituting Eq. (A4) into Eq. (A5), we obtain

$$S_{vmp} \propto N_{sss} N_{ovt} N_{probe} \sigma^* \sigma_{ovt} \sigma_{OH} (l^3 / V_{ovt}^2) \rho_0 . \tag{A6}$$

Similar considerations for the single photon dissociation ex-

periment at 246 nm give

$$S_{246} \propto N_{246} N_{\text{probe}} \sigma_{246} \sigma_{\text{OH}} (l^2/V_{246})\, \rho_0 . \qquad \text{(A7)}$$

Taking the ratio of expressions (A6) and (A7) and solving for σ^* produces

$$\sigma^* = (S_{\text{vmp}}/S_{246})(N_{246}/N_{355}N_{\text{ovt}}) \times (\sigma_{246}/\sigma_{\text{ovt}})(V_{\text{ovt}}^2/V_{246})\, l^{-1} \qquad \text{(A8)}$$

from which we calculate σ^* using the measured signals and laser pulse energies. The values for the cross section ($\sigma_{246} = 2.1\times10^{-20}$ cm^2) and ($\sigma_{\text{ovt}} = 1\times10^{-23}$ cm^2) were obtained from Refs. 28 and 27, respectively. For these cross section measurements the diameters for the vibrational overtone and 246 nm laser beams were measured to be 2 and 1 mm, respectively, and the interaction length l was estimated to be 2.5 cm.

[1] S. R. Leone, Adv. Chem. Phys. **50**, 255 (1982); J. P. Simons, J. Phys. Chem. **88**, 1287 (1984).

[2] P. F. Zittle and D. D. Little, J. Chem. Phys. **72**, 5900 (1980); P. Andresen, V. Beushausen, D. Hausler, and H. W. Lulf, J. Chem. Phys. **83**, 1429 (1985); R. Schinke, V. Engle, P. Andresen, D. Hausler, and G. G. Balint-Kurti, Phys. Rev. Lett. **55**, 1180 (1985); P. F. Zittel and D. E. Masturzo, J. Chem. Phys. **85**, 4362 (1986).

[3] D. J. Kligler, H. Pummer, W. K. Bischel, and C. K. Rhodes, J. Chem. Phys. **69**, 4652 (1978); W. K. Bischel, J. Bokor, J. Dallarosa, and C. K. Rhodes, *ibid.* **70**, 5593 (1979); S. I. Ionov, and V. N. Bagratashvili, Chem. Phys. Lett. **146**, 596 (1988); V. N. Bagratashvili, S. I. Ionov, A. A. Stuchebrukhov, V. S. Letokhov, V. N. Lokhman, and G. N. Makarov, *ibid.* **146**, 599 (1988).

[4] G. Herzberg, *Molecular Spectroscopy and Molecular Structure* (Van Nostrand Reinhold, New York, 1966), Vol. III.

[5] (a) A. Sinha, R. L. Vander Wal, L. J. Butler, and F. F. Crim, J. Phys. Chem. **91**, 4645 (1987); (b) T. M. Ticich, M. D. Likar, H. R. Dubal, L. J. Butler, and F. F. Crim, J. Chem. Phys. **87**, 5820 (1987); (c) M. D. Likar, A. Sinha, T. M. Ticich, R. L. Vander Wal, and F. F. Crim, Ber. Buns. Phys. Chem. **92**, 289 (1988); (d) M. D. Likar, J. E. Baggott, A. Sinha, T. M. Ticich, R. L. Vander Wal, and F. F. Crim, J. Chem. Soc. Faraday Trans. 2, **84**, 1483 (1988); (e) M. D. Likar, J. E. Baggott, and F. F. Crim, J. Chem. Phys. **90**, 366 (1989).

[6] L. J. Butler, T. M. Ticich, M. D. Likar, and F. F. Crim, Phys. **85**, 2331, 6251 (1986).

[7] (a) F. Biaume, J. Photochem. **2**, 139 (1973–74); (b) H. Johnston and R. J. Graham, J. Phys. Chem. **77**, 62 (1973).

[8] L. E. Harris, Nature **243**, 103 (1973); J. Chem. Phys. **58**, 5615 (1973).

[9] S. Zabarnick, J. W. Fleming, and A. P. Baronavski, J. Chem. Phys. **83**, 3395 (1986).

[10] J. August, M. Brouard, and J. P. Simons, J. Chem. Soc. Faraday Trans. 2 **84**, 587 (1988); J. August, M. Brouard, M. P. Docker, A. Hodgson, C. J. Milne, and J. P. Simons, Ber. Bunsenges, Phys. Chem. **92**, 264 (1988).

[11] A. Jacobs, K. Kleinermanns, H. Kuge, and J. Wolfrum, J. Chem. Phys. **79**, 3162 (1983).

[12] Preliminary single photon photolysis measurements in our laboratory using 200 nm photons find a smaller ratio of about 1.5. Although not as large as the ratio measured by Jacobs *et al.*, this value still differs significantly from that obtained in the work of August *et al.* using 280 nm photons and in our measurements using 241 nm photons. These differences are likely to arise from the participation of different electronic states.

[13] E. S. McGinley and F. F. Crim, J. Chem. Phys. **85**, 5741 (1986); T. M. Ticich, T. R. Rizzo, H. R. Dubal, and F. F. Crim, *ibid.* **84**, 1508 (1986).

[14] M. Suto and L. C. Lee, J. Chem. Phys. **81**, 1294 (1984), have shown that nitric acid has a relatively large absorption cross section ($\sigma \sim 1.5\times10^{-17}$ cm^2) in the region of 120 nm. This is consistent with our observation of strong emission from OH($A\,^2\Sigma^+$) produced by two-photon dissociation of nitric acid when we use a tightly focused 241 nm laser beam.

[15] H. Okabe, *Photochemistry of Small Molecules* (Wiley, New York, 1978).

[16] M. L. Sage and J. Jortner, Adv. Chem. Phys. **47**, 293 (1981); M. S. Child and L. Halonen, *ibid.* **57**, 1 (1984); B. R. Henry, Acc. Chem. Res. **10**, 207 (1977); Vib. Spectra Struct. **10**, 269 (1981).

[17] S. A. Stern, J. T. Mullhaupt, and W. B. Kay, Chem. Rev. **60**, 185 (1960); G. E. McGraw, D. L. Bernitt, and I. C. Hisatsune, J. Chem. Phys. **42**, 237 (1965).

[18] A. Sinha, R. L. Vander Wal, and F. F. Crim, J. Chem. Phys. (submitted).

[19] H. Cohn, C. K. Ingold, H. G. Poole, J. Chem. Soc. **1952**, 4272.

[20] A. P. Cox and J. M. Riveros, J. Chem. Phys. **42**, 3106 (1965).

[21] J. T. Yardley, *Introduction to Molecular Energy Transfer* (Academic, New York, 1980).

[22] We assume that both the linewidth of the transition and the probe laser are Gaussian and use the expression $\Delta\nu_D = (\Delta\nu^2 + \Delta\nu_L^2)^{1/2}$ to determine the deconvoluted linewidth $\Delta\nu_D$ from the measured width $\Delta\nu$ and the laser linewidth $\Delta\nu_L$. The linewidth of the ultraviolet probe laser is 0.4 cm^{-1}.

[23] J. L. Hardwick and J. C. Brand, Chem. Phys. Lett. **21**, 458 (1973); J. C. Brand, J. L. Hardwick, R. J. Pirkle, and C. J. Seliskar, Can. J. Phys. **51**, 2184 (1973).

[24] M. H. Alexender *et al.*, J. Chem. Phys. **89**, 1749 (1988).

[25] C. H. Greene and R. N. Zare, J. Chem. Phys. **78**, 6741 (1983); Annu. Rev. Phys. Chem. **33**, 119 (1982).

[26] In the polarization studies of the two-color vibrationally mediated photodissociations, the relative polarization of the vibrational overtones (λ_1) and photolysis (λ_2) lasers are always parallel and rotate together relative to the electric field of the probe laser.

[27] F. F. Crim, Annu. Rev. Phys. Chem. **35**, 657 (1984).

[28] NASA Panel for Data Evaluation, Chemical Kinetics and Photochemical Data for use in Stratospheric Modeling, Evaluation No. 7, JPL Publication 85-37, 1985.

[29] H. S. Johnston, S. G. Change, and G. Whitten, J. Phys. Chem. **78**, 1 (1974).

[30] The present cross section is larger than the preliminary estimate given in Ref. 5(a). This discrepancy results from the presence of background two-photon signal generated by the photolysis laser (355 nm) which led to an error in the cross section measurement in our earlier study.

[31] Using a tightly focused overtone laser beam we have also observed one-color vibrationally mediated photodissociation of nitric acid at 755 nm. This observation also supports the notion that vibrational excitation enhances the absorption cross section since the reported single photon cross section at 377 nm is negligibly small (see Refs. 7 and 26).

[32] Y. Y. Bai and G. A. Segal, J. Chem. Phys. (to be published).

[33] E. Glendenning and F. A. Weinhold (private communication). SCF/3-21G calculations were performed on $HONO_2$, OH, and NO_2 at their experimental equilibrium geometries.

[34] C. F. Jackels and E. R. Davidson, J. Chem. Phys. **65**, 2941 (1976).

[35] M. Brouard, M. T. Martinez, J. O'Mahony, and J. P. Simons (to be published); Chem. Phys. Lett. **150**, 6 (1988).